August 2019

Applied Symmetry for Crystal Structure Prediction

Scott William Fredericks
swf767@gmail.com

Repository Citation

Fredericks, Scott William, "Applied Symmetry for Crystal Structure Prediction" (2019). *UNLV Theses, Dissertations, Professional Papers, and Capstones*. 3723.
https://digitalscholarship.unlv.edu/thesesdissertations/3723

APPLIED SYMMETRY FOR CRYSTAL STRUCTURE PREDICTION

By

Scott Fredericks

Bachelor of Science in Physics
University of Arkansas, Fayetteville
2011

A thesis submitted in partial fulfillment
of the requirements for the

Master of Science - Physics

Department of Physics and Astronomy
College of Sciences
The Graduate College

University of Nevada, Las Vegas
August 2019

UNLV | GRADUATE COLLEGE

Thesis Approval

The Graduate College
The University of Nevada, Las Vegas

July 10, 2019

This thesis prepared by

Scott Fredericks

entitled

Applied Symmetry for Crystal Structure Prediction

is approved in partial fulfillment of the requirements for the degree of

Master of Science - Physics
Department of Physics and Astronomy

Qiang Zhu, Ph.D.
Examination Committee Chair

Ashkan Salamat, Ph.D.
Examination Committee Member

Tao Pang, Ph.D.
Examination Committee Member

Hui Zhao, Ph.D.
Graduate College Faculty Representative

Kathryn Hausbeck Korgan, Ph.D.
Graduate College Dean

Abstract

This thesis presents an original open-source Python package called PyXtal (pronounced "pi-crystal") that generates random symmetric crystal structures for use in crystal structure prediction (CSP). The primary advantage of PyXtal over existing structure generation tools is its unique symmetrization method. For molecular structures, PyXtal uses an original algorithm to determine the compatibility of molecular point group symmetry with Wyckoff site symmetry. This allows the molecules in generated structures to occupy special Wyckoff positions without breaking the structure's symmetry. This is a new feature which increases the space of search-able structures and in turn improves CSP performance.

It is shown that using already-symmetric initial structures results in a higher probability of finding the lowest-energy structure. Ultimately, this lowers the computational time needed for CSP. Structures can be generated for any symmetry group of 0, 1, 2, or 3 dimensions of periodicity. Either atoms or rigid molecules may be used as building blocks. The generated structures can be optimized with VASP, LAMMPS, or other computational tools. Additional options are provided for the lattice and inter-atomic distance constraints. Results for carbon and silicon crystals, water ice crystals, and molybdenum clusters are presented as usage examples.

Acknowledgements

I would first like to thank my advisor, Dr. Qiang Zhu, for his help in completing this Masters program. I sincerely appreciate his guidance and understanding, and his willingness to take me on as a student. I'd like to thank my good friends Piyush and David for their friendship, and for making these two years more enjoyable. Finally, I'd like to thank my mother and sister for their continued love and support.

Scott Fredericks

University of Nevada, Las Vegas
August 2019

Table of Contents

List of Figures

Chapter 1

Introduction: Crystal Structure Prediction and PyXtal

The key to understanding a material's properties lies in its atomic structure. If the structure is known, then almost any property can be ascertained through simulation, calculation, or some other method. In some cases the structure can be determined through experimental techniques such as X-ray diffraction or Raman spectroscopy [1]. However, this can be a costly and time-consuming process, and researchers may not have access to the necessary equipment. Furthermore, it is often impossible to perform experiments on materials which have yet to be synthesized, or which only exist at extremely high pressures and/or temperatures. The modern solution to this problem is Crystal Structure Prediction (CSP). The basic idea of CSP is to guess the correct crystal structure for specific conditions by computationally sampling a wide range of possible structures. After many attempts, the most energetically stable structure found is the one most likely to exist.

Using CSP, it is possible to discover new materials which have not yet been created. As the number of known materials grows, scientists and engineers gain new options for implementing new physical phenomena. For example, the discovery of the photovoltaic effect allowed the invention of solar-powered electricity. But in order to work, the electrons in a solar cell must be able to gain an energy level when exposed to sunlight. In practice, this means the material used must have specific electronic properties, and different materials will produce different results. For any given application there is a trade off between properties, so there is often no single ideal material. Thus, the discovery of new materials has the potential to reduce costs and improve performance in multiple industries. As a result, CSP is a growing field of active research.

A typical CSP algorithm works as follows: First, a set of random structures is generated. Different constraints can be applied (regarding the stoichiometry, lattice, symmetry, etc.) which limit the search space. Next, the structures are optimized for low energy. This involves calculating the inter-atomic forces within the crystal, then iteratively relaxing the structure until the forces cancel out. Simple force-field models are easier to calculate, but produce less accurate results. More advanced techniques like Density Functional Theory (DFT) take much longer, but in return give higher physical accuracy. After many generations, the lowest-energy structure is likely to be found, at least in theory. Further global optimization techniques such as genetic algorithms and machine learning can also be used to speed up the process [2].

While CSP is generally faster than experimental trial and error, it is still computationally expensive. Improvements at any step in the process have the potential to significantly cut costs and to allow more materials to be discovered. To this end, the author has co-developed (with his advisor Dr. Qiang Zhu) an open-source Python package called PyXtal to handle the structure generation step.

It has been shown [3] that by beginning with already-symmetric structures, fewer attempts are needed to find the global energy minimum. In PyXtal, the symmetry constraints are further refined in two main ways. The first is a merging algorithm [4] which controls the distribution of Wyckoff positions through statistical means. The second is a new algorithm for placing molecules into special Wyckoff positions. This allows for more realistic and complex structures to be generated without reducing the global symmetry.

PyXtal is not a complete CSP package; it only generates the initial structures with a given symmetry group. Other tools exist which perform structure generation and other steps in the CSP process. The main goals in developing PyXtal were: 1) to handle molecular Wyckoff positions in a generalized manner, 2) to demonstrate that proper symmetry considerations lead to better predictive results, and 3) to develop a free, open-source Python package for the materials science community.

Access to the source code and development information are available on the GitHub page at https://github.com/qzhu2017/PyXtal

Chapter 2

Background: Symmetry of Atomic Structures

2.1 Transformation Operations

Crystals are primarily categorized by their spatial symmetry. Mathematically, an object's symmetry is the group of transformations which leave its geometric structure invariant. For atomic structures, the transformations in question are those of 3D space itself: translations, rotations, and inversion. Collectively, these are called orthogonal transformations. All of these transformations preserve angles and lengths. With the exception of inversion, all can be physically applied by simply moving the structure around in real space.

When a transformation operation is applied repeatedly, the final result is sometimes the identity operation. That is, the object's final state is the same as its original state. The number of times an operation must be applied to obtain the identity is called its order. For example, the identity operation has order 1, reflections have order 2, and rational rotations have integer order. A randomly chosen transformation will probably never return the object to its original state; thus such an operation is said to have infinite order.

Because any combination of orthogonal transformations results in another orthogonal transformation, the set of all orthogonal transformations forms a mathematical group called the orthogonal group. The tools of group theory simplify the study of transformations and symmetry, as they allow for concise notation and calculations [5].

2.2 Symmetry Operations

Sometimes, applying a transformation will cause no detectable change to an object. Such a transformation is called a symmetry operation. For example, if you rotate a cube by 90 degrees about one of its faces, it will look the same; thus the 90 degree rotation is called a symmetry operation of the cube.

Any given object will have some set of symmetry operations. Because symmetry operations leave the object unchanged, that set is actually a group. This is called the object's symmetry group, and is a subgroup of the orthogonal group.

When speaking of symmetry, it is important to clearly define what constitutes equivalence between objects. In reality, two atoms may or may not be considered distinguishable based on their spin and other properties. Typically in crystallography, atoms of the same species with structurally identical environments are treated as indistinguishable. This means that if a transformation maps every atom onto another atom of the same species, that transformation is considered a symmetry operation, and the structure is effectively unchanged [6].

2.3 Periodic Symmetry

The defining feature of a crystal is the presence of periodic symmetry. This means that certain translation vectors, when applied, leave the crystal structure unchanged. For a 3D crystal, one could choose 3 such vectors. If these vectors are linearly independent, they are known as lattice vectors, and they form a parallelepiped-shaped substructure called the unit cell. The contents of a unit cell can be repeatedly "tiled" along its lattice vectors in order to reproduce the rest of the crystal (see figure 2.1).

The choice of a unit cell is not unique. Given some unit cell, one can arbitrarily choose 3 new vectors from linear combinations of the original lattice vectors. If the new vectors are again linearly independent, they will form a new unit cell. Thus there are an infinite number of possible unit cell choices. Additionally, it is possible to choose any point in the structure as the origin. For certain space groups, particularly those with multiple centers of inversion symmetry, there is no single "preferred" choice of origin. But typically, the origin will fall on the location of an atom or symmetry element. This makes the specification of the symmetry operations simpler.

Nevertheless, certain cell choices are more convenient than others. Because a different choice of unit cell will result in a different description for the structure, crystallographers have developed

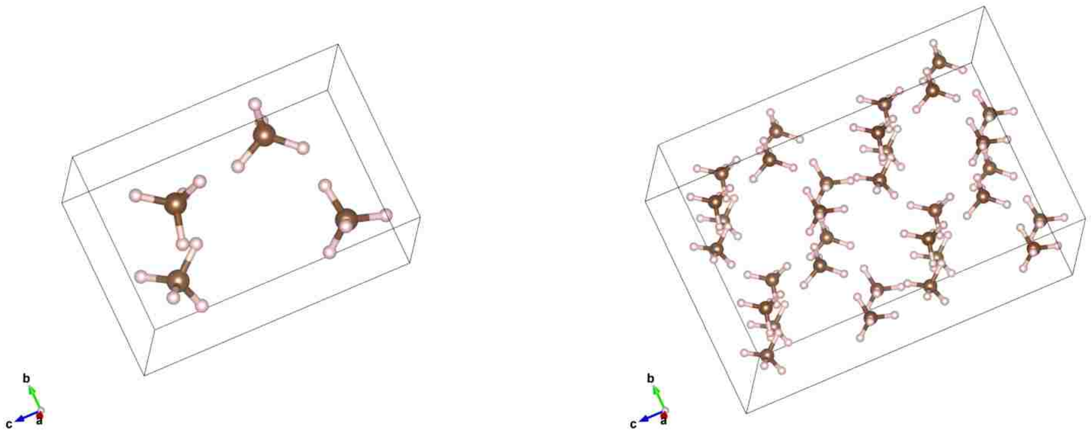

(a)

(b)

Figure 2.1: Unit Cell Example. a) The unit cell of a randomly generated methane crystal. b) a 2x2x2 supercell created by copying and translating the original unit cell along its 3 axes.

a set of standard “conventional” unit cell choices. These are the choices used by PyXtal, and are outlined in the International Tables of Crystallography, section 2.1.1 [7].

2.4 Point Group Symmetry

Crystals may also possess point group symmetry. The relevant operations are represented by orthogonal 3x3 matrices. If a matrix has determinant 1, then the operation is purely rotational, whereas a matrix with determinant -1 also involves the application of inversion. Such transformations are called roto-inversions. A symmetry group containing only rotations, reflections, and inversions is called a point group, because it always leaves at least one point in 3D space unmoved.

Because molecules are finite in size and have a well-defined position, they can possess no translational symmetry. Thus, point groups are used for studying molecular symmetry and structure.

Because a rotation can have arbitrary or infinite order, there are an infinite number of point groups. However, most of them are not relevant for crystallography or chemistry. `PyXtal` has 56 pre-generated point groups which can be chosen for cluster generation. Any other point group can be specified and generated on the fly using its Schoenflies symbol.

2.5 Symmetry Groups in Three Dimensions

A symmetry group can be artificially divided into its translational part (called the t-subgroup) and its roto-inversional component (the point group, or k-subgroup). Because a lattice is not always invariant under rotations, not every point group can be found in objects with translational symmetry. For the 3D case, there are only 32 point groups which are compatible with a lattice. These are called the crystallographic point groups, and every crystal possesses one of these as its k-subgroup.

In accordance with the crystallographic restriction theorem [8], 3D crystals may only possess 1, 2, 3, 4, or 6-fold rotational symmetry. Other orders of rotation are not compatible with 3 dimensions of periodicity. However, 5-fold symmetry has been observed in the diffraction pattern of quasicrystals [9]. These structures do not possess exact translational symmetry, but still have some long-range order. The description of such structures deviates from standard group theory, and is thus beyond the scope of PyXtal. However, some tools do exist for the analysis of quasicrystals [10].

If a symmetry group includes 3D lattice symmetry, it is called a space group. Groups with only 2 lattice vectors are called layer groups, and groups with 1 lattice vector are called Rod groups. There are 230 unique space groups, 80 layer groups, and 75 Rod groups. These, along with point groups, are the symmetry groups used by PyXtal for generating structures.

2.6 Wyckoff Positions

When the operations of a symmetry group are applied to a randomly chosen atomic position, that atom can be thought of as being repeated in space. This results in a number of copies equal to the order of the symmetry group. The generated set of atoms is then symmetric under the operation which was applied.

However, point group operations always map certain positions back onto themselves. This high-symmetry location can be a point, line, plane, or 3D space (3D space occurring only for the identity operation), and is called the symmetry element of the operation. As a result, atoms lying on symmetry elements will be mapped back onto themselves, and will thus not be copied by every operation. The symmetrically unique symmetry elements of a symmetry group are called Wyckoff positions (WP's). A WP which includes all of space is called the general position; all others are called special Wyckoff Positions [11].

The term “Wyckoff position” refers not necessarily to a single point, but to a set of points generated by the symmetry group. As an example, the space group Pmmm has order 8. Its general WP contains 8 atoms, but these 8 atoms are collectively referred to as a single WP (see figure 2.2). Furthermore, because each point in the WP is symmetrically equivalent, one can refer to the entire position using only a single coordinate. The number of symmetrically equivalent points in a Wyckoff position is called its multiplicity. WP’s reduce the amount of information needed to describe a crystal, provided the symmetry group is known. The CIF (Crystallographic Information File) file format uses this method and only stores one atom per Wyckoff position, while the POSCAR file format (used by VASP) stores each atom separately [12] [13]. As a result, CIF files tend to be smaller than POSCAR files for crystals with large unit cells. On the other hand, reading from the CIF format requires the generation of the remaining points using the symmetry group information. This exemplifies an inherent trade-off in the representation of symmetric information.

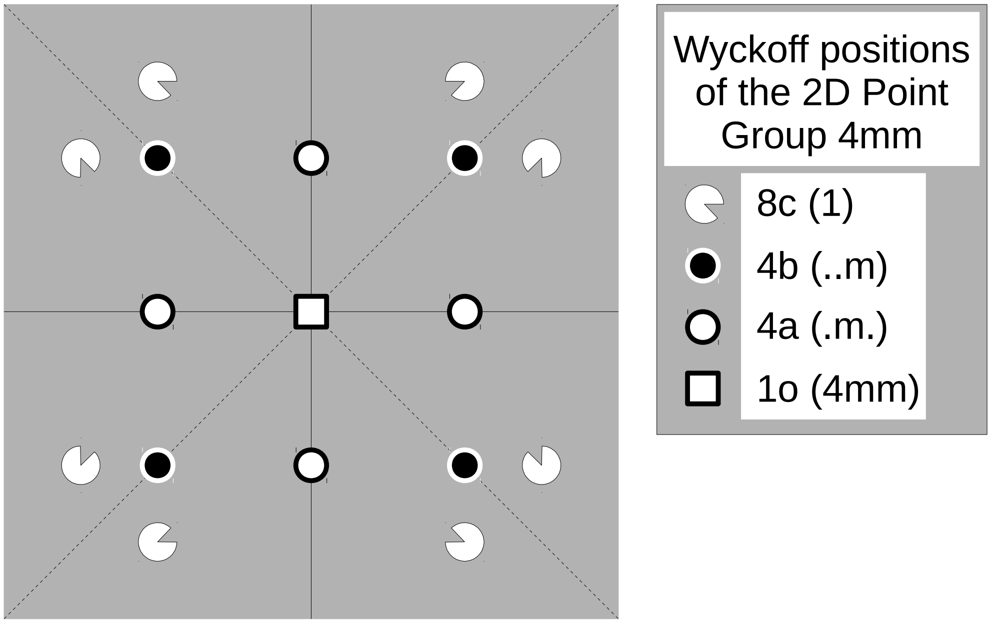

Figure 2.2: Wyckoff Positions of the Square Group 4mm. The 2D point group 4mm contains all planar symmetries of the square. Here, the solid and dashed lines mark the 4 reflectional symmetry elements. Present but not marked is a 4-fold rotational symmetry about the center. The different shapes are examples of objects in the 4 Wyckoff positions 8c, 4b, 4a, and 1o, with 8c being the general position. Different shapes of the same kind belong to a single Wyckoff position.

The subgroup of operations which maps a WP onto itself is called its site symmetry. For atomic crystals, a WP’s site symmetry only determines which 3D positions an atom can lie within. For molecular crystals, however, the site symmetry also limits which kinds of molecules can lie within certain WP's. For example, if a WP has site symmetry 2/m (a two-fold rotation accompanied by a reflection), then any molecule in that position must also have 2/m as a subgroup of its point group. Additionally, the molecule must be oriented in such a way that its relevant symmetry axes are in the same orientation as the symmetry axes of the WP (see figure **??**).

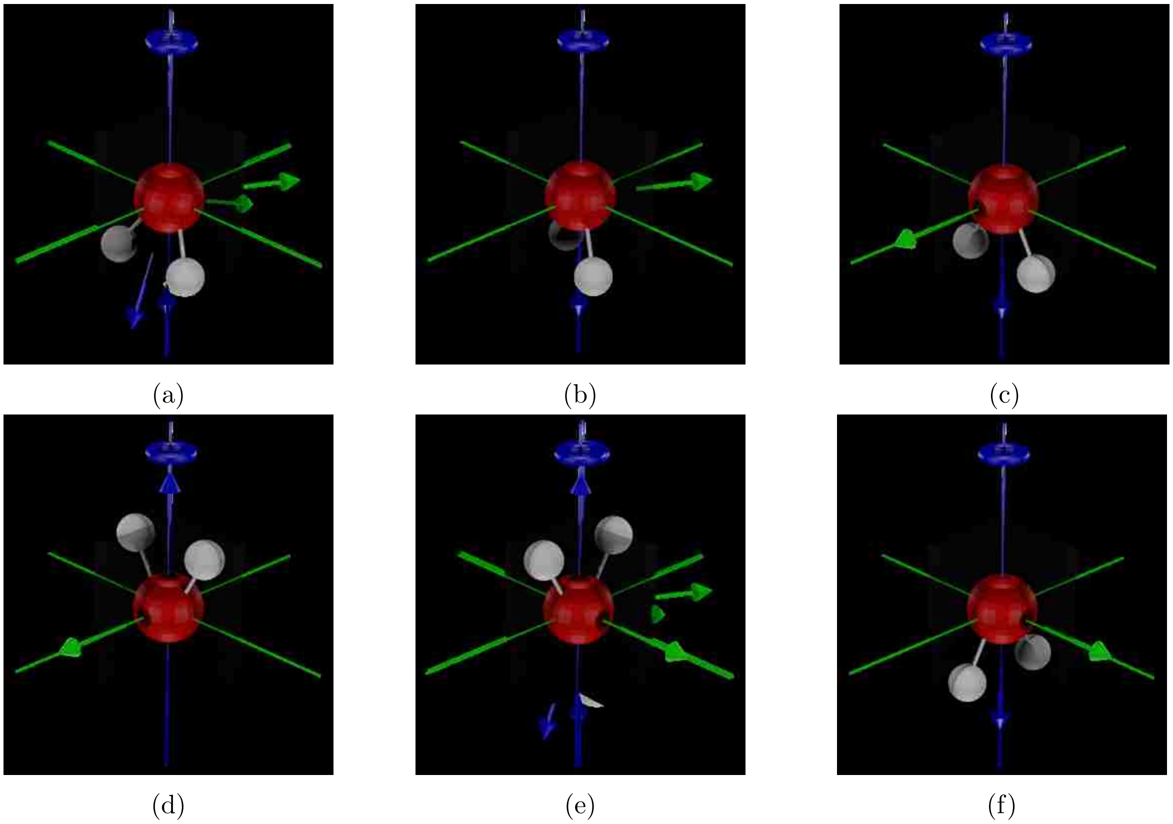

(a) (b) (c)

(d) (e) (f)

Figure 2.3: Orientations of Water in a Wyckoff Position. The planes and non-pointed axes represent the symmetry elements of a Wyckoff position with site symmetry mm2. Each plane represents a reflectional symmetry, and the blue-ringed axis represents a 2-fold rotational symmetry. (a) a water molecule with random orientation, (b) the water molecule after its rotation symmetry axis (blue, pointed) is aligned with the corresponding site symmetry rotation element, (c) the water molecule after one of its reflectional axes (green, pointed) is aligned with the corresponding site symmetry reflection element, (d)-(f) the 3 remaining valid and unique molecular orientations.

Every symmetry group has a unique set of WP's. To refer to a specific WP within a group, crystallographers use both a letter (called the Wyckoff letter) and the multiplicity. The letter increases alphabetically as the multiplicity goes up. Common examples of WP names include 1a, 2b, 4e, or 8g, but different groups will have different names for their WP's. It is worth noting that a different choice of unit cell or origin can result in different descriptions of the WP's as well. Typically, the letter-number combination refers to a WP in a standard conventional space group setting.

In a sense, all of the information about a group is stored in its WP's. In fact, a structure with a given symmetry group can be thought of as a collection of WP's with different objects in them. This is precisely the approach used by PyXtal for structure generation. If atoms are only allowed to exist in a group's WP's, then the resulting structure is guaranteed to have that group's symmetry, regardless of how many atoms are added.

2.7 Fractional Coordinates and Periodic Boundary Conditions

When working with atomic positions in a crystal, it is common to use a coordinate system based on the unit cell, rather than Euclidean space. Such coordinates are called fractional coordinates. For example, the fractional coordinate (0.0, 0.25, 0.5) would lie on the 0-plane of the a-axis, 1/4 of the way along the b-axis, and 1/2 of the way along the c-axis. The Euclidean coordinates would depend on the shape of the lattice.

Because crystals are periodic along integer translations of their unit cell axes, a single fractional coordinate actually refers to an infinite lattice of equivalent points. For most purposes, any fractional coordinate less than 0 or greater than 1 will be translated by integer values until it lies between (0,0,0) and (1,1,1).

When working with crystals computationally, it is important to remember that any object within the unit cell is actually an infinite lattice of equivalent objects. This is especially relevant for distance calculations, as discussed in later sections.

2.8 Computer Representations of Symmetry Information

Any orthogonal transformation can be described by the combination of a 3x3 orthogonal matrix (which describes the orientation) and a 3-vector (which describes the translation). One can transform a 3-vector (x, y, z) into a new vector (x', y', z') by first applying a rotation matrix M, and then adding a translation vector v:

$$\begin{bmatrix} M_{11} & M_{12} & M_{13} \\ M_{21} & M_{22} & M_{23} \\ M_{31} & M_{32} & M_{33} \end{bmatrix} \begin{bmatrix} x \\ y \\ z \end{bmatrix} + \begin{bmatrix} v_1 \\ v_2 \\ v_3 \end{bmatrix} = \begin{bmatrix} x' \\ y' \\ z' \end{bmatrix}$$

However, one can simplify this operation by representing the transformation and the original 3-vector using "augmented" 4x4 matrices [14]. Here, the 3x3 matrix and 3x1 vector are placed into a single 4x4 matrix, with 0's and a 1 on the bottom row:

$$\begin{bmatrix} M_{11} & M_{12} & M_{13} \\ M_{21} & M_{22} & M_{23} \\ M_{31} & M_{32} & M_{33} \end{bmatrix}, \begin{bmatrix} v_1 \\ v_2 \\ v_3 \end{bmatrix} \rightarrow \begin{bmatrix} M_{11} & M_{12} & M_{13} & v_1 \\ M_{21} & M_{22} & M_{23} & v_2 \\ M_{31} & M_{32} & M_{33} & v_3 \\ 0 & 0 & 0 & 1 \end{bmatrix}$$

With this notation, it becomes clear that one must define both orientation and position. But as a result, operations can be applied using standard matrix multiplication:

$$\begin{bmatrix} M_{11} & M_{12} & M_{13} & v_1 \\ M_{21} & M_{22} & M_{23} & v_2 \\ M_{31} & M_{32} & M_{33} & v_3 \\ 0 & 0 & 0 & 1 \end{bmatrix} \begin{bmatrix} O_{11} & O_{12} & O_{13} & x \\ O_{21} & O_{22} & O_{23} & y \\ O_{31} & O_{32} & O_{33} & z \\ 0 & 0 & 0 & 1 \end{bmatrix} = \begin{bmatrix} O'_{11} & O'_{12} & O'_{13} & x' \\ O'_{21} & O'_{22} & O'_{23} & y' \\ O'_{31} & O'_{32} & O'_{33} & z' \\ 0 & 0 & 0 & 1 \end{bmatrix}$$

Here, the 3x3 matrix O represents the original orientation of the object being transformed, and O' is the new orientation.

For symmetric objects, orientations are ambiguous by definition. Atoms, which are assumed to be spherically symmetric, do not have a well-defined orientation, because there is no way to distinguish which way an atom is "facing". More generally, a single orientation for a symmetric object actually corresponds to a group of orientations which is conjugate to the object's symmetry group.

For example, consider an object with reflection symmetry. If a random orientation is chosen, then there is always one other orientation (the mirror image) which is indistinguishable from the original orientation. Thus, the number of unique orientations is half as large as it would be for an asymmetric object. In general, as the symmetry group grows, the space of unique orientations shrinks. A group-theoretic representation of orientation would thus use a different size of object depending on the size of the symmetry group. Indeed, in quantum mechanics the symmetry of particles directly influences their statistical behavior. A well-known example is that the number of degrees of freedom for a molecule changes its thermodynamic properties.

For PyXtal's purposes, it suffices to simply store an object's orientation matrix and its symmetry operations. Comparisons between orientations can still be performed algorithmically this way.

In certain cases, particularly when using special Wyckoff positions, one may want to apply singular transformations. For example, one may want to place a randomly located atom into the Wyckoff position (0,0,z). In this case, the position is effectively 1-dimensional, despite existing within 3D space. The solution is to project the original coordinate onto the symmetry element represented by the Wyckoff operator.

As another example, consider the symmetry element (x,x,0), which is a diagonal axis running through the z-plane. If the original point were (0.9,0.1,0.0), then the projected point on the axis would be (0,0,0) due to periodic boundary conditions.

In practice, coordinates can be generated for any Wyckoff position by simply applying the Wyckoff position's 4x4 matrices to an arbitrary 3-vector. However, to ensure an even distribution of points in 3D space, one must first find the closest projection of the point onto the symmetry element. So, a Wyckoff position can be thought of as a set of 4x4 matrices, and a space group can be thought of as a set of Wyckoff positions. The storage, interpretation, and arithmetic for the 4x4 matrices is currently handled by Pymatgen's SymmOp class [15].

Because non-integer matrix multiplication depends on floating point operations, numerical accuracy is a legitimate concern. To check for equivalence, it is useful to define some cutoff difference tolerance. If all matrix values are equal within this tolerance, then matrices are considered equal. Because PyXtal only works with groups of order less than a few hundred, this accuracy is sufficient. For groups of very high order, one might instead use quaternions or other calculation methods with higher numerical accuracy.

Chapter 3

The Structure Generation Algorithm

3.1 Overview

PyXtal follows the same basic algorithm for each type of structure which can be generated. First, the user inputs their choice of dimension (0, 1, 2, or 3), symmetry group, stoichiometry, and relative volume of the unit cell. Optionally, additional parameters may be chosen which constrain the unit cell and maximum inter-atomic distance tolerances. This is implemented through the random_crystal and molecular_crystal Python classes. Next, PyXtal checks to make sure the stoichiometry is compatible with the choice of symmetry group. If the check passes, then generation begins. Figure 3.1 shows a flowchart of the algorithm.

Each remaining step has a maximum number of attempts. If generation fails at any point, the algorithm will revert progress for the current step and try again, until the maximum attempt limit has been reached. This ensures that the algorithm stops in finite time, while still giving each generated parameter a chance for success. For certain inputs, generation may take many attempts or fail after the maximum number of attempts. Typically, these failures indicate that the input parameters are not likely to produce a realistic structure without fine-tuned atomic positions. In such cases, a larger unit cell or smaller distance tolerances may improve the chances of successful generation.

3.2 Wyckoff Compatibility Checking

Before attempting to generate a structure, PyXtal must make sure it is possible to do so. The WP's in different space groups have different multiplicities. As a result, not every number of atoms is compatible with every space group. For example, consider the space group Pn-3n (#222). The

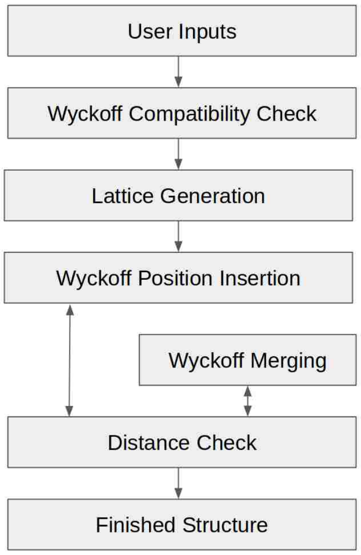

Figure 3.1: PyXtal Structure Generation Flowchart. Generation is based on inputs from the user.

smallest Wyckoff position is 2a, with the next smallest being 6b. It is impossible to create a crystal with 4 atoms in the unit cell for this symmetry group, because no combination of Wyckoff positions adds up to 4. The position 2a cannot be repeated, because it falls on the exact coordinates (1/4, 1/4, 1/4) and (3/4, 3/4, 3/4). A second set of atoms in the 2a position would overlap the atoms in the first position, but this is not physically possible.

Thus, it is necessary to check the input stoichiometry against the Wyckoff positions of the desired space group. To accomplish this, PyXtal iterates through all possible Wyckoff position combinations within the confines of the stoichiometry. As soon as one valid combination is found, the check returns true. If no valid combination is found, the check returns false, and the generation attempt fails with a warning.

Some space groups allow valid combinations of WP's, but may not give many degrees of freedom for generation. It may also be the case that the allowed combinations result in atoms which are too close together. In these cases, PyXtal will attempt generation as usual: until the maximum limit is reached, or until a successful generation occurs. If generation repeatedly fails for a given combination of space group and stoichiometry, the user should make note and avoid the combination going forward.

3.3 Lattice Generation

The first step in PyXtal's structure generation is the choice of unit cell. Depending on the symmetry group, a specific type of lattice must be generated. For all crystals, the conventional cell choice is used to avoid ambiguity. The most general case is the triclinic cell, from which other cell types can be obtained by applying various constraints.

To generate a triclinic cell, 3 real numbers are randomly chosen (using a Gaussian distribution centered at 0) as the off-diagonal values for a 3x3 shear matrix. Treating this matrix as a cell matrix, one obtains 3 lattice angles. For the lattice vector lengths, a random 3-vector between (0,0,0) and (1,1,1) is chosen (using a Gaussian distribution centered at (0.5,0.5,0.5)). The relative values of the x, y, and z coordinates are used for a, b, and c respectively, and scaled based on the required volume.

For other cell types, any free parameters are obtained using the same methods as for the triclinic case, along with any necessary constraints. In the tetragonal case, for example, all angles must be 90 degrees. Thus, only a random vector is needed to generate the lattice constants.

3.4 Wyckoff Position Selection and Merging

The central building block for crystals in PyXtal is the Wyckoff position (WP). Once a space group and lattice are chosen, WP's are inserted one at a time to add structure.

PyXtal starts with the largest available WP, which is the general position of the space group. If the number of atoms required is equal to or greater than the size of the general position, the algorithm proceeds. If fewer atoms are needed, the next largest WP (or set of WP's) is chosen, in order of descending multiplicity. This is done to ensure that larger positions are preferred over smaller ones; this reflects the greater prevalence of larger multiplicities both statistically and in nature.

Once a WP is chosen, a random 3-vector between (0,0,0) and (1,1,1) is created. This acts as the generating point. Projecting this vector into the WP, one obtains a set of coordinates in real space. Then, the distances between these coordinates are checked. If the atom-atom distances are all greater than a pre-defined limit, the WP is kept and the algorithm continues. If any of the distances are too small, it is an indication that the WP would not occur with that generating point. In this case, the coordinates are merged together into a smaller WP, if possible. This merging continues until the atoms are no longer too close together (see figure 3.2).

To merge into a smaller position, the original generating point is projected into each of the remaining WP's. The WP with the smallest translation between the original point and the transformed point is chosen, so long as the new WP is a subset of the original one, and so long as the new points are not too close together. If the atoms are still too close together, the WP is discarded and another attempt is made.

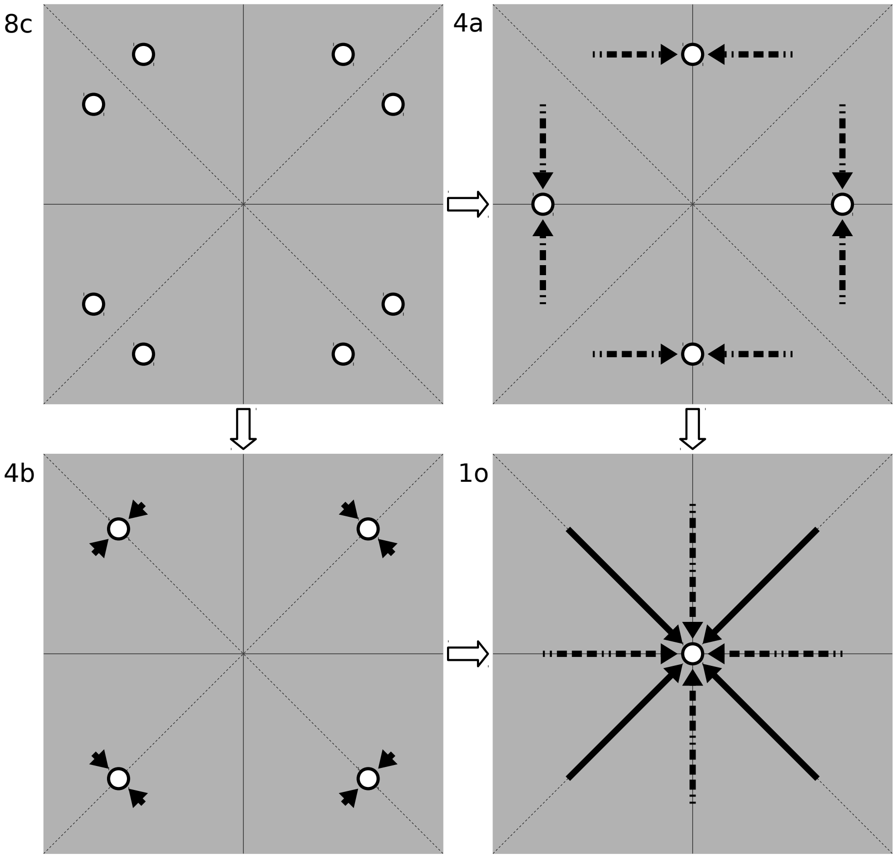

Figure 3.2: Wyckoff Position Merging Example. Shown are possible mergings of the general position 8c of the 2D point group 4mm. Moving from 8c to 4b (along the solid arrows) requires a smaller translation than for 4a (along the dashed arrows). Thus, if the atoms in 8c were too close together, PyXtal would merge them into 4b instead of 4a. The atoms could be further merged into position 1o by following the arrows shown in the bottom right image.

Once a satisfactory WP has been filled, the inter-atomic distances between the current WP and the already-added WP's are checked. If all distances are acceptable, the algorithm continues. More WP's are then added as needed until the desired number of atoms has been reached. At this point, either a satisfactory structure has been generated, or the generation has failed. If the generation fails, then either smaller distances tolerances or a larger volume factor might increase the chances of success. However, altering these quantities too drastically may result in less realistic crystals. Common sense and system-specific intuition should be applied when adjusting these parameters.

3.5 Distance Checking

To produce structures with realistic bonds and bond lengths, the generated atoms should not be too close together. In PyXtal this means that by default, two atoms should be no closer than the covalent bond length between them. However, for a given application the user may decide that shorter or longer cutoff distances are appropriate. For this reason, PyXtal has a custom tolerance matrix class which allows the user to define the distances allowed between any two types of atoms.

Because crystals have periodic symmetry, any point in a crystal actually corresponds to an infinite lattice of points. Likewise, any separation vector between two points actually corresponds to an infinite number of separation vectors. For the purposes of distance checking, only the shortest of these vectors are relevant. When a lattice is non-Euclidean, the problem of finding shortest distances with periodic boundary conditions is non-trivial, and the general solution can be computationally expensive [16]. So instead, an approximate solution is used based on assumptions about the lattice geometry:

For any two given points, PyXtal first considers only the separation vector which lies within the "central" unit cell spanning between (0,0,0) and (1,1,1). For example, if the original two (fractional) points are (-8.1, 5.2, -4.8) and (2.7, -7.4, 9.3), one can directly obtain the separation vector (-10.8, 12.6, -14.1). This is then translated to the vector (0.2, 0.6, 0.9), which lies within the central unit cell. PyXtal also considers those vectors lying within a 3x3x3 supercell centered on the first vector. These would include (1.2, 1.6, 1.9), (-0.8, -0.4, -0.1), (-0.8, 1.6, 0.9), etc. This gives a total of 27 separation vectors to consider. After converting to absolute coordinates, one can calculate the Euclidean length of each of these vectors and thus find the shortest distance.

Note that this does not work for certain vectors within some highly distorted lattices (see figure 3.3). Often the shortest Euclidean distance is accompanied by the shortest fractional distance, but whether this is the case or not depends on how distorted the lattice is. However, because all lattices are required to have no angles smaller than 30 degrees or larger than 150 degrees, this is not an issue.

For two given sets of atoms (for example, when cross-checking two WP's in the same crystal), one can calculate the shortest inter-atomic distances by applying the above procedure for each

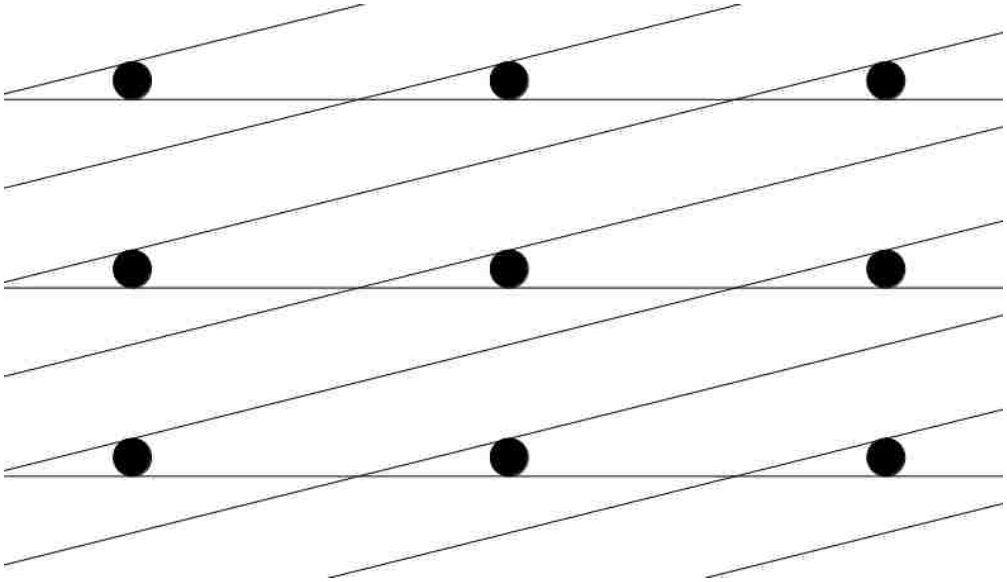

Figure 3.3: Distorted Unit Cell. Due to the cell's high level of distortion, the closest neighbors for a single point lie more than two unit cells away. In this case, the closest point to the central point is located two cells to the left and one cell diagonal-up. To find this point using PyXtal's distance checking method, a 5x5x5 unit cell would be needed. For this reason, a limit is placed on the distortion of randomly generated lattices.

unique pair of atoms. This only works if it has already been established that both sets on their own satisfy the needed distance requirements.

Thanks to symmetry, it is not necessary to calculate every atomic pair between two Wyckoff positions. For two Wyckoff positions A and B, one need only calculate either the separations between one atom in A and all atoms in B, or one atom in B and all atoms in A. This is because the symmetry operations which duplicate a point in a Wyckoff position also duplicate the separation vectors associated with that point. This is also true for a single Wyckoff position; for example, in a Wyckoff position with 16 points, only 16 calculations are needed, as opposed to 256. This can significantly speed up the calculation for larger Wyckoff positions.

For a single WP, it is necessary to calculate the distances for each unique atom-atom pair, but also for the lattice vectors for each atom by itself. Since the lattice is the same for all atoms in the crystal, this check only needs to be performed on a single atom of each specie. For atomic crystals, this just means ensuring that the generated lattice is sufficiently large.

For molecules, the process is slightly more complicated. Depending on the molecule's orientation within the lattice, the inter-atomic distances can change. Additionally, one must calculate the distances not just between molecular centers, but between every unique atom-atom pair. This increases the number of needed calculations, in rough proportion to the square of size of the molecules. As a result, this is typically the largest time cost for generation of molecular crystals.

The issue of checking the lattice is also dependent on molecular orientation. Thus, the lattice must be checked for every molecule in the crystal. To do this, the atoms in the original molecule are checked against the atoms in periodically translated copies of the molecule. Here, standard atom-atom distance checking is used.

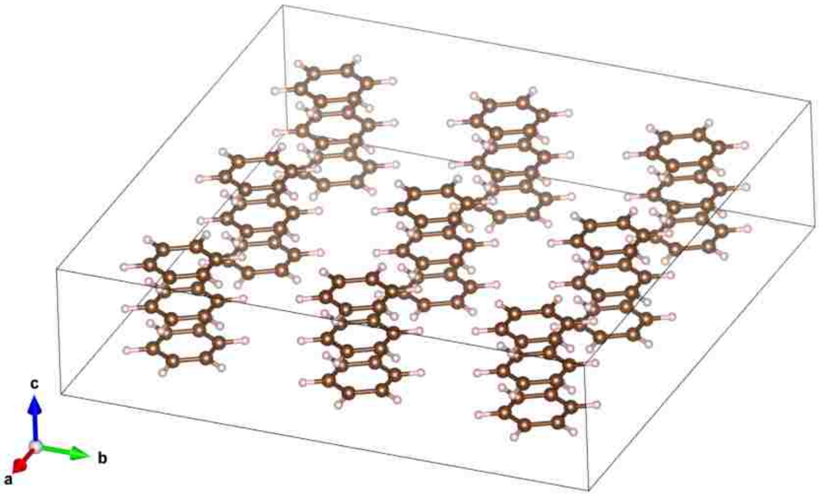

Figure 3.4: Dependence of Shortest Distances on Molecular Orientation. Rotation about the a or b (but not the c) axes would cause the benze molecules to overlap. PyXtal checks for overlap whenever a molecular orientation is altered.

While several approximate methods for inter-molecular distance checking exist, their performance is highly dependent on the molecular shape and on the number of atoms in the molecule. The simplest of these is to simply model the molecule as a sphere, in which only the center-center distances are needed. This works well for certain molecule like buckminsterfullerene, which has a large number of atoms and is approximately spherical in shape. But it works poorly for irregularly shaped molecules like benzene, which can have short separations along its perpendicular axis, but must be further apart along in-plane axes. So, this is left as an option for the user; direct atom-atom distance checking is used by default.

3.6 Molecular Orientations

In crystallography, atoms are typically assumed to be point particles with no well-defined orientation. Since the object occupying a crystallographic Wyckoff position is usually an atom, it is further assumed that the object's symmetry group contains the Wyckoff position's site symmetry as a subgroup. If this is the case, the only remaining condition for occupation of a Wyckoff position is the location within the unit cell. However, if the object is instead a molecule, then the Wyckoff position compatibility is also determined by orientation and shape.

To handle the general case, one must ensure that the object 1) is sufficiently symmetric, and 2) is oriented such that its symmetry operations are aligned with the Wyckoff site symmetry. The result is that different point group symmetries are compatible with only certain Wyckoff positions. For a given molecule and Wyckoff position, one can find all valid orientations as follows:

1. Determine the molecule's point group and point group operations. This is currently handled by Pymatgen's build-in PointGroupAnalyzer class, which produces a list of symmetry operations for the molecule.

2. Associate an axis to every symmetry operation. For now, it can be assumed that the axis is centered at the origin. For a rotation or improper rotation, use the rotational axis. For a mirror plane, use an axis perpendicular to the plane. Note that inversional symmetry does not add any constraints, since the inversion center is always located at the molecule's center of mass.

3. Find up to two non-collinear axes in the site symmetry and calculate the angle between them. Find all conjugate operations (with the same order and type) in the molecular point symmetry with the same angle between the axes, and store the rotation which maps the pairs of axes onto each other. For example, if the site symmetry were mmm, then choose two reflectional axes, say the x and y axes or the y and z axes. Then, look for two reflection operations in the molecular symmetry group. If the angle between these two operation axes is 90 degrees, store the rotation which maps the two molecular axes onto the Wyckoff axes for every pair of reflections with 90 degrees separating them.

4. For a given pair of axes, there are two rotations which can map one onto the other, with opposite directions of the molecular axis. Depending on the molecular symmetry, these two rotations may produce the same molecular orientation. Using the list of rotations calculated in step 3, remove redundant orientations which are equivalent to each other.

5. For each found orientation, check that the rotated molecule is symmetric under the Wyckoff

site symmetry. To do this, simply check the site symmetry operations one at a time by transforming the molecule and checking for equivalence with the untransformed molecule.

6. For the remaining valid rotations, store the rotation matrix and the number of degrees of freedom. If two axes were used to constrain the molecule, then there are no degrees of freedom. If one axis is used, then there is one rotational degree of freedom, and store the axis about which the molecule may rotate. If no axes are used (because there are only point operations in the site symmetry), there are three (stored internally as two) degrees of freedom, meaning the molecule can be rotated freely in 3 dimensions.

PyXtal performs these steps for every Wyckoff position in the symmetry group and stores the nested list of valid orientations. When a molecule must be inserted into a Wyckoff position, an allowed orientation is randomly chosen from the list. This forces the overall symmetry group to be preserved, because symmetry-breaking positions are not allowed.

It is worth noting that the general position of any symmetry group always has site symmetry group 1. This means that any molecule can always be inserted into the general position with any orientation. However, many real crystals have molecules located in special positions, and thus this method alone is insufficient for generating realistic structures [17].

Another important consideration is whether a symmetry group will produce inverted copies of the constituent molecules. In many cases, a chiral molecule's mirror image will possess different chemical or biological properties [18]. For pharmaceutical applications in particular, one may not want to consider crystals containing mirror molecules. By default, PyXtal does not generate crystals with mirror copies of chiral molecules. The user can choose to allow inversion if desired.

Chapter 4

Results

4.1 Point group clusters

To demonstrate the general utility of pre-symmetrization, random molybdenum clusters were generated and optimized using the Lennard-Jones potential model [19]. Finding the ground state for a cluster of given size is an established benchmark for global optimization methods [20]. Here, it shown that local optimization, combined with PyXtal's pre-symmetrization, are sufficient to solve the problem. Clusters were generated of size 38, 55, and 75. For each cluster size, 20,000 structures were generated: 10,000 with no pre-defined symmetry, and 10,000 with symmetry chosen randomly from among PyXtal's 56 built-in point groups. A potential of $4(\frac{1}{r^{12}} - \frac{1}{r^{6}})$ was assigned to each atom-atom pair. Each structure was locally optimized using SciPy's optimize.minimize function [21], using the conjugate gradient (CG) method. As shown in the following figures, the ground state was found much more frequently when the initial structures possessed some point group symmetry. With pre-symmetrization, the ground state was found 170 times for size 38 clusters, 254 times for size 55, and 1 time for size 75. Without pre-symmetrization, the ground state was not found at all.

It is worth noting that while the ground state is found more frequently with pre-symmetrization, the average energy is higher. This are several possible contributing factors. First, the energy distribution is generally broader for the pre-symmetrized structures. This suggests that pre-symmetrization spans the possible structure space more effectively, while asymmetric structures are more clustered around a specific energy range. Because finding all structures at least once is more important than finding somewhat low-energy structures multiple times, pre-symmetrization seems the clear choice for energy optimization.

The probability of finding the ground state is clearly influenced by cluster size, though the exact relationship is unclear from these results. There seem to be at least two competing factors as the cluster size increases: the increasing expected level of symmetry in the ground state, and the increasing space of possible structures. In other words, the probability of finding the ground state naturally goes down with increasing cluster size, but the probability of the ground state having high symmetry increases. As a result, the net probability would be the highest for intermediate-sized clusters. More cluster sizes and larger samples would help make any such trends more apparent.

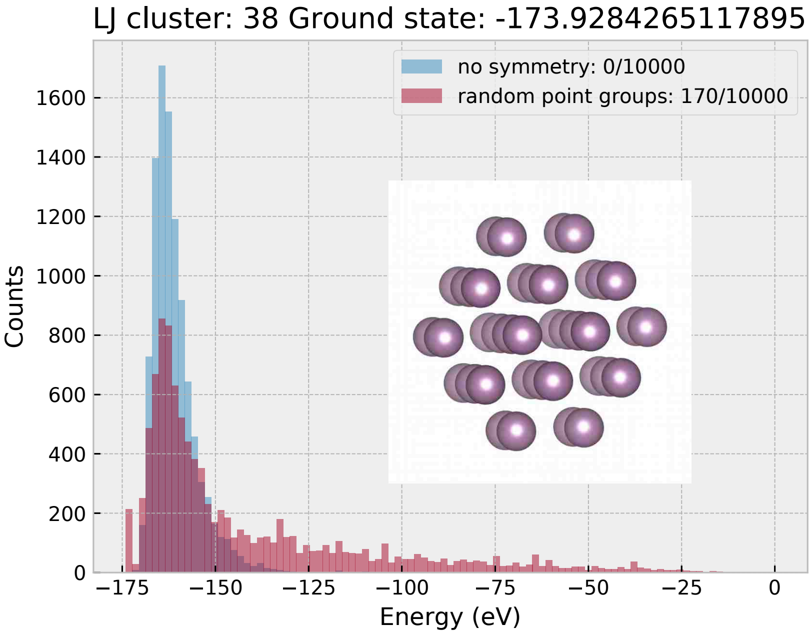

Figure 4.1: Energy distribution for Lennard Jones size 38 Clusters. The pre-symmetrized structures produce a wider range of energies, reaching nearly all the way up to 0 eV. However, pre-symmetrization also produces more structures at the lowest energies.

4.2 Carbon and Silicon Crystals

A separate test was performed to find the ground states for Carbon and Silicon at 0 K and 0 Pa. For both elements, 1000 random structures each were generated for 2, 4, 6, 8, and 16 atoms in the primitive cell. A random space group between 2 and 230 was chosen for each structure. This gave a total of 5000 structures for each element. Each structure was optimized using VASP [22, 23, 24, 25], and the final energy was calculated using a single point energy calculation (see appendices B-D for exact settings). Finally, similar structures were grouped using Pymatgen's StructureMatcher tool with a fractional length tolerance of .05, site tolerance of 0.1, and angular tolerance of 5.0 degrees.

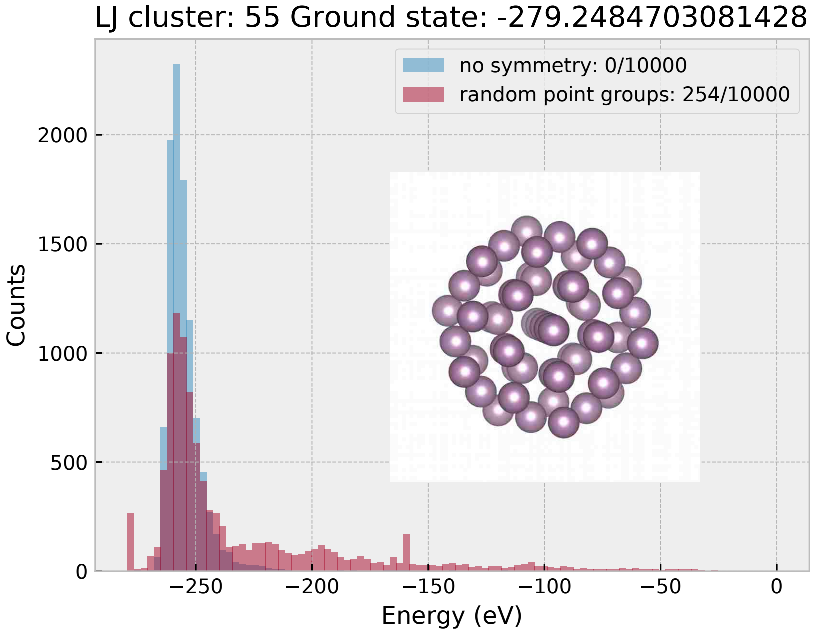

Figure 4.2: Energy distribution for Lennard Jones size 55 Clusters. The distribution is similar to that of size 38, but the ground state is found more frequently. This suggests that symmetry may become increasingly important for larger structures.

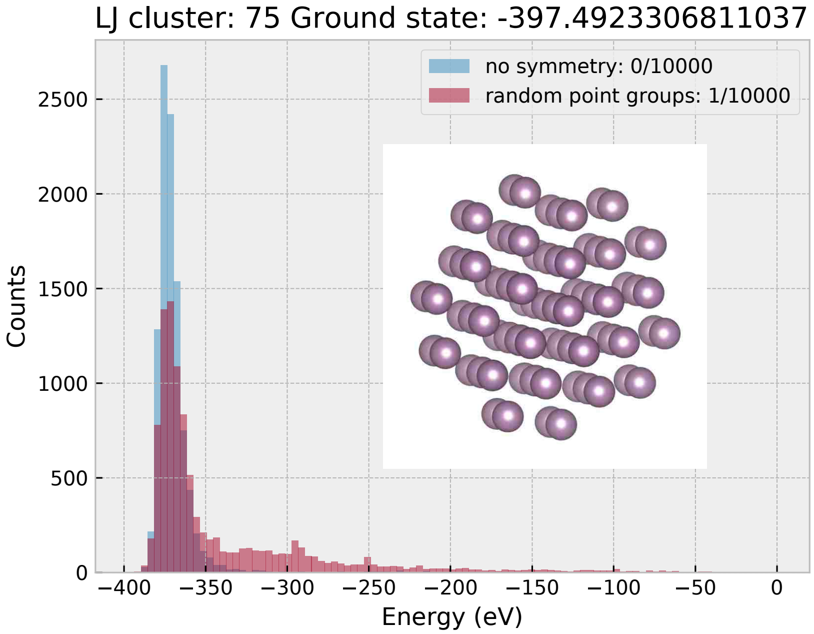

Figure 4.3: Energy distribution for Lennard Jones size 75 Clusters. The ground state was only found once, making extrapolation difficult. The distribution shape is similar to those of size 38 and 55.

A total of 2542 unique structures were found for Carbon, and 2306 for Silicon.

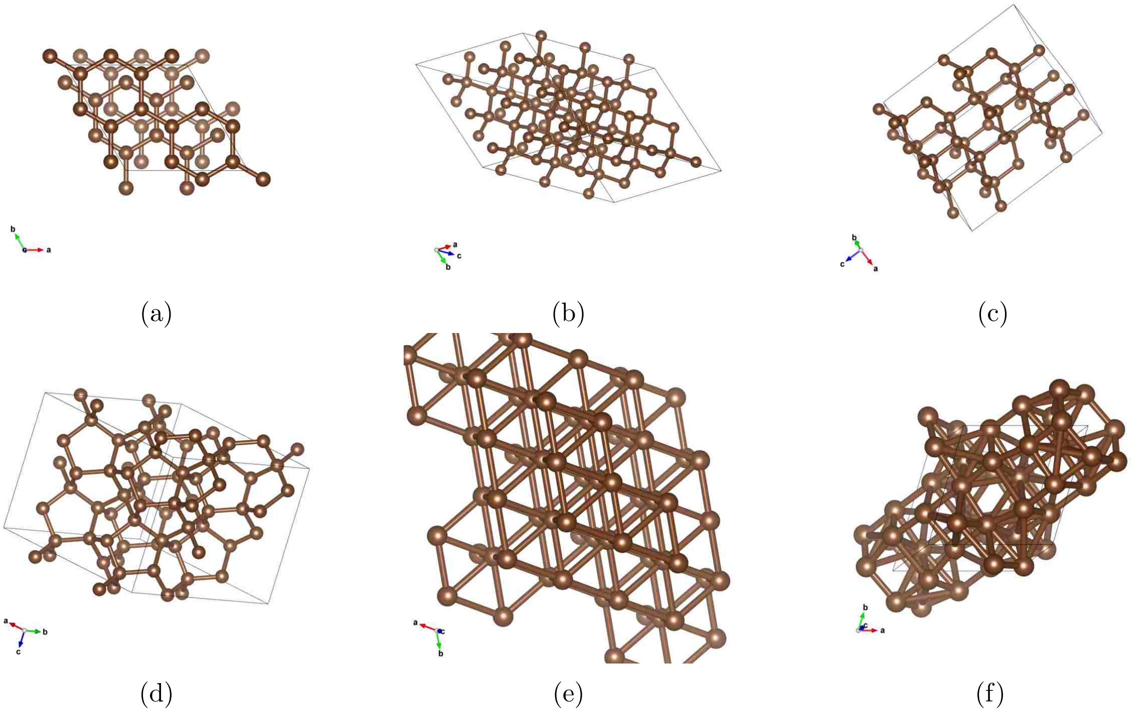

(a) (b) (c)

(d) (e) (f)

Figure 4.4: Representative Carbon Structures. These include (a) a graphite-like structure (-9.226 eV/atom), (b) diamond (-9.099 eV/atom), (c) lonsdaelite (-9.068 eV/atom), (d) a low-energy pentagonal structure also found for silicon (-8.984 eV/atom), (e), a mid-energy structure (-5.888 eV/atom), (f) a high-energy structure (-0.009 eV/atom)

For Carbon, the expected structures of diamond and graphite were found, as well as londsdaelite and various multi-layer graphene structures. The graphene-based structures were not well-differentiated by energy: there were many slightly different structures varying only by the displacements between their layers. As a result, these structures were not grouped together by pymatgen. A prototypical example is shown in figure 4.4. By comparison, most of the remaining structures appeared to be well-ranked. Structures with higher energies typically had less realistic bond structures than those with lower energies, and were either too dense or not dense enough.

However, because the lowest energy structures are the most important, a better ranking method would be useful for further studies. More accurate relaxation methods and energy calculations would hopefully 1) reduce the number of similar but slightly perturbed structures, and 2) make the ranking of low-energy structures easier and more accurate. It is clear that systems with weaker forces between atoms are more sensitive to small changes in energy. This is apparent from the multi-layer graphene structures, for which the differentiating degrees of freedom involved weak layer-layer forces, and also from the results for water ice (described in the next section).

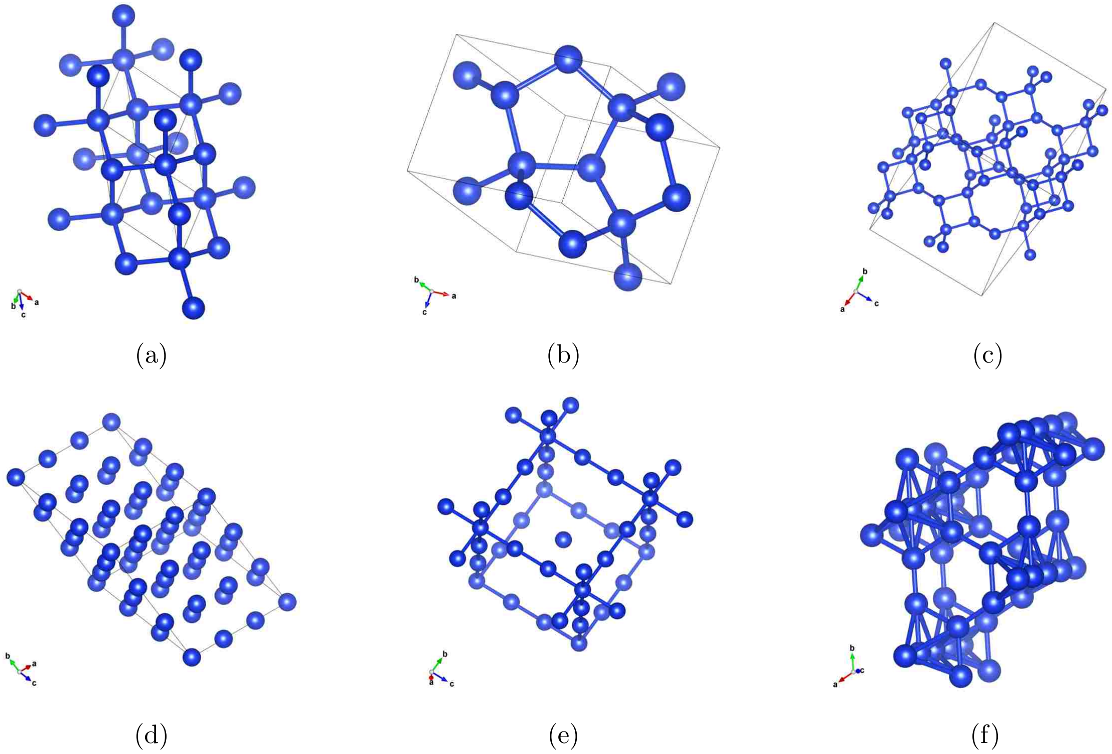

(a) (b) (c)

(d) (e) (f)

Figure 4.5: Representative Silicon Structures. These include (a) diamond cubic (-5.423 eV/atom), (b) a pentagonal structure (-5.372 eV/atom), (c) another low-energy structure (-5.319 eV/atom), (d) a mid-energy structure with a simple lattice (-4.933 eV/atom), (e) a sparse high-energy structure (-3.488 eV/atom), and (f) a dense high-energy structure (-0.072 eV/atom)

For Silicon, the diamond cubic structure was found many times and had the lowest energy. In contrast to carbon, there is a rich variety of geometries among the unique lowest-energy structures. Because most of these structures are based on distorted polygonal rings, it is difficult to tell them apart without the use of a structure matching tool. However, fewer total unique structures were found than were for carbon. Additionally, pymatgen was able to more effectively group similar Silicon structures together. Overall, Silicon appears to have fewer stable structures than Carbon. Because the allotropes of Silicon are less well-studied than those of Carbon, it is difficult to tell how accurate the energy rankings are. More accurate calculations would likely be required to do so.

Figure 4.6b shows the distribution of lattice energies for the final optimized structures. A few trends are apparent. First, Silicon is more heavily skewed towards the ground state energy than Carbon. Additionally, the standard deviation for Silicon is smaller. Both of these details suggest that Silicon has a smaller space of possible low-energy structures. This is expected, since Carbon

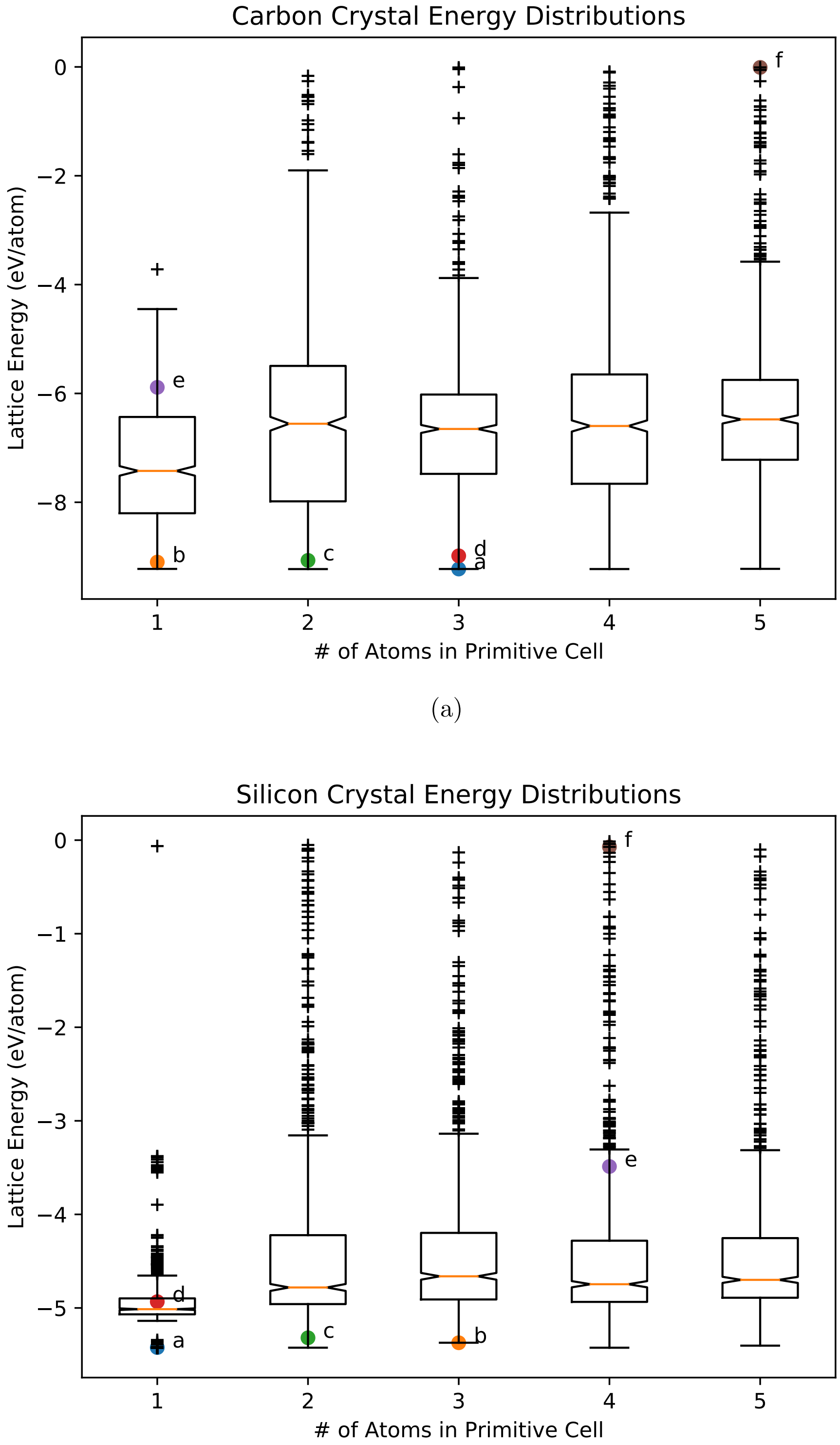

(a)

(b)

Figure 4.6: Lattice Energy Distributions for Carbon and Silicon. The structures from figures 4.4 and 4.5 are marked with colored circles. ”+” symbols represent outliers. ($\pm 2.7\sigma$). Structures with positive lattice energies are not included.

is known for its ability to form multiple bonds of different types, which in turn should allow it to form more kinds of stable structures.

Second, the energy landscape appears to be smaller for size-2 primitive cells. It appears that beyond about 4, the number of atoms in the primitive cell has little influence on the energy distribution. For Carbon and Silicon, the diamond cubic structure has only 2 atoms in its primitive cell. Thus, it makes sense that increasing the number of atoms would not improve the chances of finding the ground state. For more complex stoichiometries, it is likely that larger unit cells would produce better results, since more unique structures would exist for higher-order symmetry groups. Here, the consistency in energy shows that few new structures are being found for larger primitive cells. This also suggests that larger Wyckoff positions are not typically stable for single-atom systems. It is possible that different atomic systems would feature large Wyckoff positions more frequently. Further study is needed to determine which properties influence the average Wyckoff position size.

4.3 3D Ice

A final test was performed for water ice crystals. Random H_2O crystals were generated using PyXtal with between 1 and 4 molecules in the primitive cell. Each structure was then optimized using a force-field model in LAMMPS (see appendix A for exact settings) [26]. Optimization was implemented using the materials science Python package ASE [27]. First the FIRE [28] method was performed, followed by the BFGS [29] method, with a maximum allowed force of 0.001 kcal/(mol-Angstrom), and a maximum of 1000 steps for each method. If the optimized structure had a stress value less than 0.001 atm, it was kept. A total of 1000 such optimized structures were generated.

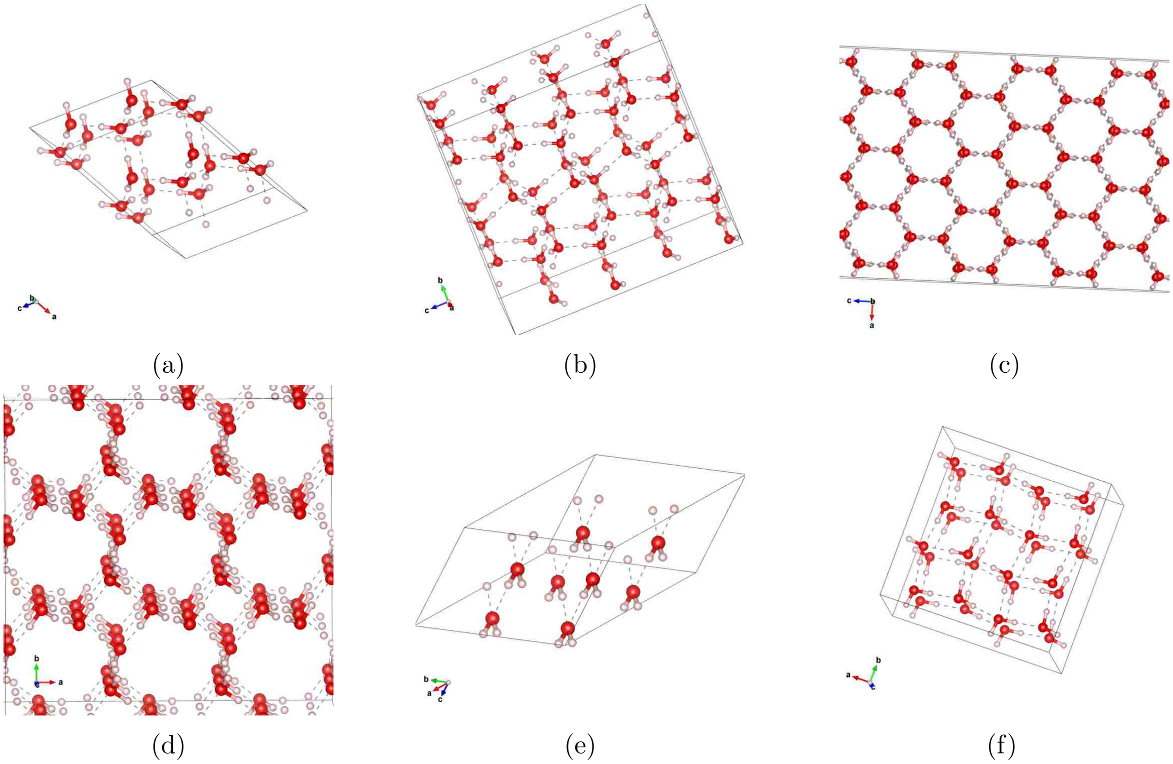

(a) (b) (c) (d) (e) (f)

Figure 4.7: Representative Ice Structures. (a) cubic ice with a distorted lattice (-14.879 eV/-molecule), (b) A hexaxgonal oxygen structure with different hydrogen bonds (-14.875 eV/molecule), (c) standard ice with distorted oxygen positions (-14.869 eV/molecule), (d) a mid-energy structure (-14.788 eV/molecule), (e) a high-energy layered structure (-14.515 eV/molecule), (f) a different high-energy layered structure (-14.495 eV/molecule)

To avoid redundant calculations, similar structures were grouped together using Pymatgen's StructureMatcher tool, again with with a fractional length tolerance of .05, site tolerance of 0.1, and angular tolerance of 5.0 degrees. This brought the number of unique structures to 275.

It is worth noting that at this point, some the known polymorphs of water ice could already be recognized. In order to accurately rank the results though, density function theory (DFT) calculations are necessary. This is because force-field models do not take quantum effects or electron structure into account, and thus the calculated energies are not accurate.

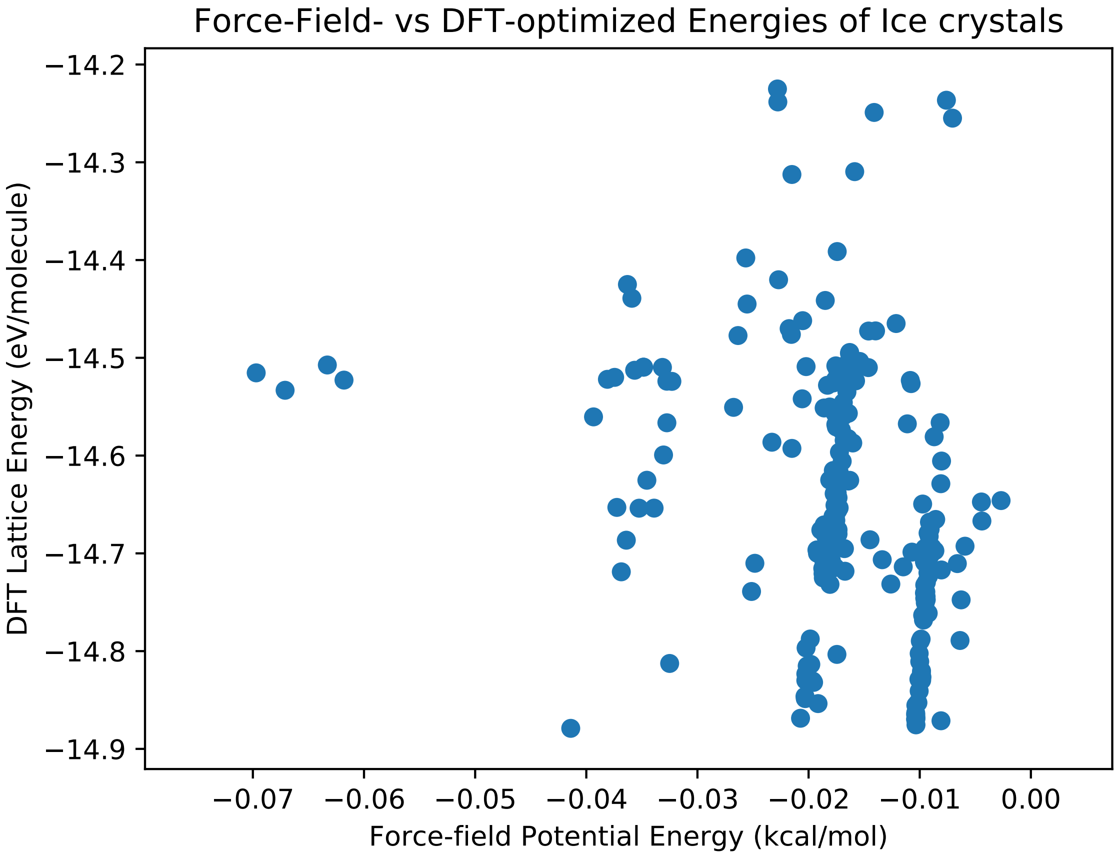

Figure 4.8: Energy Distribution for H_2O Crystals. There is very little correlation between the DFT and Force-field energies. However, there are clear vertical line clusters near -0.01 and -0.02 on the x-axis.

Next, DFT optimization was performed using VASP (see appendices B, C, and D for exact settings). Two steps of optimization were performed with increasing accuracy, followed by a single point energy calculation. Some of the original and resulting structures had unrealistic geometries, such as improper O-H bond structures or unreasonably large or small inter-molecular distances. Such structures were removed, leaving 227 final structures.

The final structures were ranked based on their single point energy. Six representative structures are shown in figure 4.7. Standard water ice was found, though it was not the lowest energy structure, and was very slightly distorted from the expected geometry. Many similar structures were found which were not considered equivalent by the StructureMatcher tool; as a result, it is difficult to determine exactly how often each structure type appeared. The top-ranking structures which are sufficiently similar to the shown structures are not included.

It is known that molecular crystal polymorphs are often very close energetically [30]. This makes ranking difficult, because the difference in energies between structures may be less than the accuracy of the computation methods. More importantly, multiple polymorphs may be metastable at a given temperature and pressure. As seen in Figure 4.8, there is no clear trend relating the force-field and single point energies. This shows that the force-field energy alone is insufficient for accurate ranking.

However, there are two or three clusters of lines near -0.01 and -0.02 on the x-axes. These lines are slightly slanted upward to the right. Because the points on these lines are so close together, it is likely that they belong to the same structural prototypes. If this is the case, then it appears that small changes in the Force-field energy resulted in relatively large changes in the final DFT energy for similar structures. This suggests that the DFT calculation did not have sufficient time or accuracy for complete relaxation. If the relaxation had been sufficient, we would expect similar structures to relax to approximately the same final energy. This would result in an approximately horizontal line, which is not seen here. So, it is likely that improving the DFT accuracy would significantly improve the energy rankings and would make grouping similar structures easier.

Chapter 5

Comparison with Existing Tools

Various pieces of software exist to facilitate CSP. Although CSP will typically out-perform experimental trial and error, considerable computation time is still required. Improvements at any level of the algorithm have the potential to speed up the process by a significant factor. The primary advantage of PyXtal is its unique method of pre-symmetrization, particularly for molecular and low-dimensional crystals. This helps reduce the needed number of initial structures, and in turn the number of calculations to perform.

Furthermore, many existing software packages are either paid or usable on a license-only basis. To increase accessibility for the materials science community, PyXtal was developed as an open-source Python package. This way, anyone can use and modify the code as needed, without the need for access to special computing resources. A few free atomic simulation tools exist, including LAMMPS and Quantum Espresso, which can be used by anyone. Several other packages are free for academic users, but require registration or a license key. By combining PyXtal or another structure generation utility with open source software, it is hypothetically possible for anyone with a desktop computer to perform CSP for basic systems. PyXtal currently has interface options for LAMMPS and VASP.

Another potential advantage of PyXtal is its implementation in the Python programming language. Python is a popular language among scientists and engineers. A researcher familiar with Python can easily modify and implement the code for their specific needs. The source code, as well as detailed documentation, are readily available online. Because structure generation is typically much faster than simulation, speed is less important than for other steps in the CSP process. Thus, implementation in a low-level language or library is not as important as it is for most other scientific applications. With that said, PyXtal makes use of Numpy's vectorization at several steps in order to optimize the generation speed. For the systems tested, structure generation is significantly faster than the force-field optimization of the same structure.

Nevertheless, because PyXtal only focuses on the structure generation step of CSP, it is currently left to the user to determine which kinds of structures to generate. While advancements to machine learning are helping to automate the process, it is still advisable for a researcher to perform searches with constraints determined based on prior knowledge and assumptions. For example, if the user suspects that certain space groups are more likely to occur than others, it would be beneficial to generate more structures with those space groups. Thus, PyXtal is currently best suited for someone with both materials science and Python programming experience.

Because PyXtal is only intended as the first step in CSP, it does not perform optimization, ranking, clustering, or visualization. Users who desire a more complete CSP package and do not need PyXtal's features should consider other tools. These include, but are not limited to, USPEX [2], XtalOpt [31], GRACE [32], and CALYPSO [33].

Chapter 6

Limitations and Further Study

6.1 Crystal Structure Prediction Methods Used

For this study, a very basic CSP method was used. Random structures were generated and then optimized in an essentially trial-and-error way. The only significant improvements were PyXtal's pre-symmetrization scheme and the grouping of similar structures using Pymatgen. More advanced CSP techniques can drastically reduce the time needed to find the ground state. Such techniques might include genetic algorithms and mutations, better ranking systems, machine learning, or different optimization methods. Of course, the implementation of more advanced techniques comes with its own challenges, namely a proper software implementation and more complex background knowledge. Some of the tools mentioned in the previous section implement such techniques. However, the primary goal of this thesis is to demonstrate that PyXtal can be used for CSP in general. Because PyXtal can be called using customized Python scripts, other pieces of software could hypothetically implement it within more advanced CSP algorithms. It is the author's hope that the original features found in PyXtal will be utilized by other researchers in this way.

6.2 Complexity of the Systems Studied

The crystal systems studied in this thesis are relatively simple. A more rigorous test of PyXtal's abilities would involve finding the ground state for an unknown or very complex system. Increased complexity could involve a larger number of atoms in the unit cell, metallic atoms with more complicated valence mechanics, or more than one kind of atomic specie. The introduction of more species may necessitate a larger space of possible structures, since the stoichiometry of the ground state may not be known. For example, to determine the convex hull for a poly-atomic system, one would need to generate structures having different ratios of each atomic specie. While PyXtal is capable of generating such structures, it is up to the user to define each possible stoichiometry separately.

6.3 Molecular Flexibility

An inherent limitation of PyXtal is that molecules are assumed to be rigid; no stereoisomers of any kind are considered. For H_2O this is not an issue, because the molecule is simple enough that most perturbations will not alter the bond structure. But for larger molecules, especially those with many degrees of freedom, this approach may be insufficient. The ground state crystal could potentially have different molecular configuration or bond angles than those supplied.

The problem of pre-symmetrization becomes much more complicated when molecules are given flexibility. It is then necessary to determine whether a given perturbation will change the symmetry or not, and the resulting symmetry group must be calculated. It may be theoretically possible to analyze the symmetry of every relevant molecular geometry. However, the space of all possible configurations may be highly complex and nontrivial, which in turn would lead to more structures needing to be generated.

A partial solution would be to input multiple configurations of the molecule before generation. If the molecular configuration space is sufficiently sampled, then the molecules may be able to relax into the correct geometry during optimization. Of course, as the molecular complexity grows, the number of configuration samples would also need to grow. If more than a few degrees of freedom are present, the number could quickly grow beyond computational limits. Efficient handling of complex molecular systems remains a computationally challenging problem.

6.4 Non-crystalline Systems

Another inherent limitation of PyXtal is that it only handles classical crystal structures. This means that amorphous structures, quasi-crystals, order-disorder systems, and host-guest systems cannot be directly generated. The study of these kinds of systems would require a generalization of the mathematics used by PyXtal. For example, the treatment of quasi-crystals involves the use of hyper-dimensional symmetry groups [34], whereas PyXtal only allows for groups of 3 or fewer dimensions. It is hypothetically possible that such systems could be found during the optimization stage, provided a large enough supercell is used. But in this case, one might as well forgo symmetry and generate completely random initial structures. PyXtal is best used when the ground state is suspected to possess standard crystal symmetry.

Chapter 7

Conclusion

This thesis has covered the conceptual background for the original software package PyXtal. The core features of PyXtal have been highlighted, with further documentation available online. The primary new feature - special Wyckoff positions for molecular crystals - has been described in detail, and its usefulness has been demonstrated by quickly finding the ground state of water ice.

PyXtal, along with its source code and documentation, is currently available online at https://github.com/qzhu2017/PyXtal. Further development will continue as different needs arise.

Examples for 0D atomic, 3D atomic, and 3D molecular structures have been provided. For each case, the ground state was found within a few thousand generation attempts. This shows that PyXtal is sufficient for generating random crystal structures.

While several improvements could be made to PyXtal, its original goals have been achieved. It has been shown that proper handling of symmetry is useful for efficiently and accurately searching the energy landscape. Furthermore, the utility of symmetry groups and Wyckoff positions as a basis for hypothetical structures suggests the possibility of more fundamental representations. Further development and application of the mathematical background should enable more complex structure types to be studied in the future.

Appendix A

LAMMPS Settings Used for H_2O

```
clear
units electron
boundary p p p
atom_modify sort 0 0.0

### interactions
atom_style full
pair_style      lj/cut/tip4p/long 1 2 1 1 0.278072379 17.007
bond_style      class2
angle_style     harmonic
kspace_style pppm/tip4p 0.0001
read_data tmp/data.lammps
pair_coeff  2  2 0 0
pair_coeff  1  2 0 0
pair_coeff  1  1  0.000295147 5.96946
neighbor 2.0 bin
min_style cg
minimize 1e-6 1e-6 10000 10000
thermo_style custom pe pxx
thermo_modify flush yes
thermo 1
run 0
```

Appendix B

VASP INCAR for DFT Optimization

Step 1

```
INCAR created by Atomic Simulation Environment
 KSPACING = 0.400000
 POTIM = 0.020000
 PSTRESS = 0.000000
 EDIFF = 1.00e-02
 ALGO = normal
 GGA = PE
 PREC = low
 IBRION = 2
 ISIF = 4
 NPAR = 8
 NSW = 10
 KGAMMA = .TRUE.
 LCHARG = .FALSE.
 LWAVE = .FALSE.
```

Appendix C

VASP INCAR for DFT Optimization Step 2

```
INCAR created by Atomic Simulation Environment
 KSPACING = 0.300000
 POTIM = 0.050000
 PSTRESS = 0.000000
 EDIFF = 1.00e-03
 ALGO = normal
 GGA = PE
 PREC = normal
 IBRION = 2
 ISIF = 3
 NPAR = 8
 NSW = 25
 KGAMMA = .TRUE.
 LCHARG = .FALSE.
 LWAVE = .FALSE.
```

Appendix D

VASP INCAR for DFT Single Point Energy Calculations

```
INCAR created by Atomic Simulation Environment
 ENCUT = 600.000000
 KSPACING = 0.150000
 PSTRESS = 0.000000
 EDIFF = 1.00e-04
 GGA = PE
 PREC = accurate
 IBRION = 2
 ISIF = 3
 NPAR = 8
 NSW = 0
 KGAMMA = .TRUE.
 LCHARG = .FALSE.
 LWAVE = .FALSE.
```

Bibliography

[1] K. D. M. Harris and M. Tremayne, "Crystal structure determination from powder diffraction data," *Chemistry of Materials*, vol. 8, no. 11, pp. 2554–2570, 1996. [Online]. Available: https://doi.org/10.1021/cm960218d

[2] A. Oganov, Y. ma, C. Glass, and M. Valle, "Evolutionary crystal structure prediction: Overview of the uspex method and some of its applications," *Psi-k Newsl.*, vol. 84, 01 2007.

[3] P. Avery and E. Zurek, "Randspg: An open-source program for generating atomistic crystal structures with specific spacegroups," *Computer Physics Communications*, vol. 213, pp. 208–216, 2017.

[4] Q. Zhu, A. Oganov, C. Glass, and H. T Stokes, "Constrained evolutionary algorithm for structure prediction of molecular crystals: Methodology and applications," *Acta crystallographica. Section B, Structural science*, vol. 68, pp. 215–26, 06 2012.

[5] B. Souvignier, "Chapter 1.1. a general introduction to groups," *International Tables for Crystallography*, vol. A, pp. 2–11, 2016.

[6] H. Wondratschek and M. I. Aroyo, "Chapter 1.2. crystallographic symmetry," *International Tables for Crystallography*, vol. A, pp. 12–21, 2016.

[7] M. I. A. H. D. F. K. M. Th. Hahn, A. Looijenga-Vos and P. Konstantinov, "2.1. guide to the use of the space-group tables," *International Tables for Crystallography*, vol. A, pp. 142–144, 2016.

[8] A. Vince, "Periodicity, quasiperiodicity, and bieberbach's theorem on crystallographic groups," *The American Mathematical Monthly*, vol. 104, no. 1, pp. 27–35, 1997. [Online]. Available: http://www.jstor.org/stable/2974820

[9] D. Shechtman, I. Blech, D. Gratias, and J. W. Cahn, "Metallic phase with long-range orientational order and no translational symmetry," *Phys. Rev. Lett.*, vol. 53, pp. 1951–1953, Nov 1984. [Online]. Available: https://link.aps.org/doi/10.1103/PhysRevLett.53.1951

[10] A. Yamamoto, "Software package for structure analysis of quasicrystals. sci technol adv mater. 2008 mar 6;9(1):013001. doi," in *PubMed PMID: 27877919; PubMed Central PMCID: PMC5099788*, pp. 10–1088.

[11] M. I. A. G. C. B. Souvignier, H. Wondratschek and A. M. Glazer, "Chapter 1.4. space groups and their descriptions," *International Tables for Crystallography*, vol. A, pp. 42–74, 2016.

[12] S. R. Hall, F. H. Allen, and I. D. Brown, "The crystallographic information file (CIF): a new standard archive file for crystallography," *Acta Crystallographica Section A*, vol. 47, no. 6, pp. 655–685, Nov 1991. [Online]. Available: https://doi.org/10.1107/S010876739101067X

[13] (2019, Feb) Poscar. University of Vienna CMS. [Online]. Available: https://cms.mpi.univie.ac.at/wiki/index.php/POSCAR

[14] B. S. H. Wondratschek, M. I. Aroyo and G. Chapuis, "Chapter 1.5. transformations of coordinate systems," *International Tables for Crystallography*, vol. A, pp. 75–105, 2015.

[15] S. P. Ong, W. D. Richards, A. Jain, G. Hautier, M. Kocher, S. Cholia, D. Gunter, V. L. Chevrier, K. A. Persson, and G. Ceder, "Python materials genomics (pymatgen): A robust, open-source python library for materials analysis," *Computational Materials Science*, vol. 68, pp. 314 – 319, 2013. [Online]. Available: http://www.sciencedirect.com/science/article/pii/S0927025612006295

[16] L. Babai, "On lovász' lattice reduction and the nearest lattice point problem," *Combinatorica*, vol. 6, no. 1, pp. 1–13, Mar 1986. [Online]. Available: https://doi.org/10.1007/BF02579403

[17] U. M. ller, "3.2.4. molecular symmetry," *International Tables for Crystallography*, vol. A, p. 72776, 2016.

[18] I.-H. Suh, K. H. Park, W. P. Jensen, and D. E. Lewis, "Molecules, crystals, and chirality," *Journal of Chemical Education*, vol. 74, no. 7, p. 800, 1997. [Online]. Available: https://doi.org/10.1021/ed074p800

[19] J. E. Jones and S. Chapman, "On the determination of molecular fields.&#x2014;i. from the variation of the viscosity of a gas with temperature," *Proceedings of the Royal Society of London. Series A, Containing Papers of a Mathematical and Physical Character*, vol. 106, no. 738, pp. 441–462, 1924. [Online]. Available: https://royalsocietypublishing.org/doi/abs/10.1098/rspa.1924.0081

[20] D. J. Wales and J. P. K. Doye, "Global optimization by basin-hopping and the lowest energy structures of lennard-jones clusters containing up to 110 atoms," *The Journal of Physical Chemistry A*, vol. 101, no. 28, pp. 5111–5116, 1997. [Online]. Available: https://doi.org/10.1021/jp970984n

[21] E. Jones, T. Oliphant, P. Peterson *et al.*, "SciPy: Open source scientific tools for Python," 2001–, [Online; accessed ¡today¿]. [Online]. Available: http://www.scipy.org/

[22] G. Kresse and J. Hafner, "Ab initio molecular dynamics for liquid metals," *Phys. Rev. B*, vol. 47, pp. 558–561, Jan 1993. [Online]. Available: https://link.aps.org/doi/10.1103/PhysRevB.47.558

[23] ——, "Ab initio molecular-dynamics simulation of the liquid-metal–amorphous-semiconductor transition in germanium," *Phys. Rev. B*, vol. 49, pp. 14 251–14 269, May 1994. [Online]. Available: https://link.aps.org/doi/10.1103/PhysRevB.49.14251

[24] G. Kresse and J. Furthmller, "Efficiency of ab-initio total energy calculations for metals and semiconductors using a plane-wave basis set," *Computational Materials Science*, vol. 6, pp. 15–50, 07 1996.

[25] G. Kresse and J. Furthmüller, "Efficient iterative schemes for ab initio total-energy calculations using a plane-wave basis set," *Phys. Rev. B*, vol. 54, pp. 11 169–11 186, Oct 1996. [Online]. Available: https://link.aps.org/doi/10.1103/PhysRevB.54.11169

[26] S. Plimpton, "Fast parallel algorithms for short-range molecular dynamics," *Journal of Computational Physics*, vol. 117, no. 1, pp. 1 – 19, 1995. [Online]. Available: http://www.sciencedirect.com/science/article/pii/S002199918571039X

[27] A. H. Larsen, J. J. Mortensen, J. Blomqvist, I. E. Castelli, R. Christensen, M. Dułak, J. Friis, M. N. Groves, B. Hammer, C. Hargus, E. D. Hermes, P. C. Jennings, P. B. Jensen, J. Kermode, J. R. Kitchin, E. L. Kolsbjerg, J. Kubal, K. Kaasbjerg, S. Lysgaard, J. B. Maronsson, T. Maxson, T. Olsen, L. Pastewka, A. Peterson, C. Rostgaard, J. Schiøtz, O. Schtt, M. Strange, K. S. Thygesen, T. Vegge, L. Vilhelmsen, M. Walter, Z. Zeng, and K. W. Jacobsen, "The atomic simulation environment—a python library for working with atoms," *Journal of Physics: Condensed Matter*, vol. 29, no. 27, p. 273002, jun 2017. [Online]. Available: https://doi.org/10.1088%2F1361-648x%2Faa680e

[28] E. Bitzek, P. Koskinen, F. Gähler, M. Moseler, and P. Gumbsch, "Structural relaxation made simple," *Phys. Rev. Lett.*, vol. 97, p. 170201, Oct 2006. [Online]. Available: https://link.aps.org/doi/10.1103/PhysRevLett.97.170201

[29] J. D. Head and M. C. Zerner, "A broydenfletchergoldfarbshanno optimization procedure for molecular geometries," *Chemical Physics Letters*, vol. 122, no. 3, pp. 264 – 270, 1985. [Online]. Available: http://www.sciencedirect.com/science/article/pii/0009261485805741

[30] S. A.-E. G. B. J. B. S. G. G. H. Y. H. R. H. Y. H. A. K. K. N. A. O. C. P. B. R. R. S. W. T. S. W. C. W. X.-F. Z. Q. Z. C.S. Adjiman, A. Aspuru-Guzik, *Topics in Current Chemistry 345: Prediction and Calculation of Crystal Structures ule Atahan-EvrenkAln Aspuru-GuzikEditorsMethods and Applications*, ule Atahan-Evrenk and A. Aspuru-Guzik, Eds. Springer, 2014.

[31] D. C. Lonie and E. Zurek, "Xtalopt: An open-source evolutionary algorithm for crystal structure prediction," *Computer Physics Communications*, vol. 182, no. 2, pp. 372 – 387, 2011. [Online]. Available: http://www.sciencedirect.com/science/article/pii/S0010465510003140

[32] J. Hoja, H.-Y. Ko, M. A. Neumann, R. Car, R. A. DiStasio, and A. Tkatchenko, "Reliable and practical computational description of molecular crystal polymorphs," *Science Advances*, vol. 5, no. 1, 2019. [Online]. Available: https://advances.sciencemag.org/content/5/1/eaau3338

[33] Y. Wang, J. Lv, L. Zhu, and Y. Ma, "Calypso: A method for crystal structure prediction," *Computer Physics Communications*, vol. 183, no. 10, pp. 2063 – 2070, 2012. [Online]. Available: http://www.sciencedirect.com/science/article/pii/S0010465512001762

[34] P. M. de Wolff, T. Janssen, and A. Janner, “The superspace groups for incommensurate crystal structures with a one-dimensional modulation,” *Acta Crystallographica Section A*, vol. 37, no. 5, pp. 625–636, Sep 1981. [Online]. Available: https://doi.org/10.1107/S0567739481001447

Curriculum Vitae

Graduate College
University of Nevada, Las Vegas

Scott Fredericks
scottwfredericks@gmail.com

Degrees:

Bachelor of Science in Physics 2011
University of Arkansas, Fayetteville, AR

Thesis Examination Committee:

Chairperson, Qiang Zhu, Ph.D.
Committee Member, Dr. Ashkan Salamat, Ph.D.
Committee Member, Dr. Tao Pang, Ph.D.
Graduate Faculty Representative, Dr. Hui Zhao, Ph.D.